JVI Journals.ASM.org

A Virus-Like Particle That Elicits Cross-Reactive Antibodies to the Conserved Stem of Influenza Virus Hemagglutinin

Anette Schneemann,[a] Jeffrey A. Speir,[a] Gene S. Tan,[b] Reza Khayat,[a] Damian C. Ekiert,[a]* Yumiko Matsuoka,[c] and Ian A. Wilson[a,d]

Department of Molecular Biology, The Scripps Research Institute, La Jolla, California, USA[a]; Department of Microbiology, Mount Sinai School of Medicine, New York, New York, USA[b]; Laboratory of Infectious Diseases, National Institute of Allergy and Infectious Diseases, National Institutes of Health, Bethesda, Maryland, USA[c]; and Skaggs Institute for Chemical Biology, The Scripps Research Institute, La Jolla, California, USA[d]

The discovery of broadly neutralizing antibodies that recognize highly conserved epitopes in the membrane-proximal region of influenza virus hemagglutinin (HA) has revitalized efforts to develop a universal influenza virus vaccine. This effort will likely require novel immunogens that contain these epitopes but lack the variable and immunodominant epitopes located in the globular head of HA. As a first step toward developing such an immunogen, we investigated whether the 20-residue A-helix of the HA2 chain that forms the major component of the epitope of broadly neutralizing antibodies CR6261, F10, and others is sufficient by itself to elicit antibodies with similarly broad antiviral activity. Here, we report the multivalent display of the A-helix on icosahedral virus-like particles (VLPs) derived from the capsid of Flock House virus. Mice immunized with VLPs displaying 180 copies/particle of the A-helix produced antibodies that recognized trimeric HA and the elicited antibodies had binding characteristics similar to those of CR6261 and F10: they recognized multiple HA subtypes from group 1 but not from group 2. However, the anti-A-helix antibodies did not neutralize influenza virus. These results indicate that further engineering of the transplanted peptide is required and that display of additional regions of the epitope may be necessary to achieve protection.

The isolation of broadly neutralizing antibodies against influenza A viruses has reinforced the notion that development of a universal influenza virus vaccine is, in principle, possible (8, 9, 13, 20, 36, 39, 45). Broadly neutralizing antibodies are protective against multiple viral subtypes and generally recognize epitopes in the highly conserved membrane-proximal region of hemagglutinin (HA). This interaction inhibits infection by preventing fusion of the viral and cellular membranes (9, 12, 13, 36). In contrast, most antibodies elicited in response to the current vaccines bind to immunodominant epitopes located in the membrane-distal head of HA and prevent receptor binding and entry of the virus (2, 15–17). The HA head is highly variable, explaining the lack of protection against viruses that do not closely correspond to the vaccine strain. The specific epitopes recognized by broadly neutralizing antibodies, such as CR6261 (12), F10 (36), CR8020 (13), and FI6v3 (9), have been identified and their structures in complex with their cognate antibodies revealed by X-ray crystallography (Fig. 1A). The challenge now resides in developing antigens that present these epitopes to the immune system in a way that induces a potent and protective antibody response.

We and others have shown that icosahedral, virus-like particles (VLPs) represent highly effective platforms for the development of novel vaccines (4, 19, 21, 24, 30, 31, 38). Icosahedral virus particles are known to be strongly immunogenic based on the repetitive array of their component proteins, particulate nature, and ability to appropriately stimulate the innate immune response. By using genetic engineering and structure-based design, we have developed the T=3 icosahedral insect virus Flock House virus (FHV) as a VLP platform for multivalent presentation of foreign antigens on its surface (10, 24).

FHV particles are assembled from 180 identical copies of the coat protein, each with prominent peptide loops at amino acid positions 206 and 264, which form trimers on the particle surface (Fig. 1B) (33). These loops have been successfully utilized for genetic insertion of both foreign peptides and entire proteins up to 20 kDa in size. Using this system, we previously developed a novel vaccine against anthrax that protects rats from lethal toxin challenge 3 weeks after a single immunization in the absence of adjuvant (24).

In the present study, we investigated whether HA epitopes of broadly neutralizing antibodies against influenza virus can be displayed in their native conformation on the surface of FHV and whether the resulting antigen-presenting particles elicit antibodies with similarly broad antiviral specificity. We focused our attention on the epitope recognized by antibodies CR6261 and F10. These antibodies recognize HA subtypes in group 1 (10 of the 16 subtypes), including H1, H2, and H5, but not HA subtypes in group 2, such as H3 (36, 39). The epitope consists of a highly conserved helical segment, the A-helix, in the membrane-proximal region of the HA2 chain, and a few neighboring residues in both HA2 and HA1 chains (Fig. 1A) (12, 36). With a few exceptions, most of the HA A-helix residues contacted by the broadly neutralizing antibodies are >99% identical across all subtypes, whereas those occluded in the trimer interface are more variable (Fig. 1C). Notably, the A-helix is the major determinant for antibody recognition in terms of buried surface, accounting for 70% of the CR6261 contact area. This area also accounts for most of the polar interactions with CR6261, whereas the other adjacent residues in the epitope contribute primarily hydrophobic interac-

Received 30 June 2012 Accepted 9 August 2012

Published ahead of print 15 August 2012

Address correspondence to Anette Schneemann, aschneem@scripps.edu, or Jeffrey A. Speir, speir@scrippps.edu.

* Present address: Damian C. Ekiert, Department of Microbiology and Immunology, UC-San Francisco, San Francisco, California, USA.

doi:10.1128/JVI.01694-12

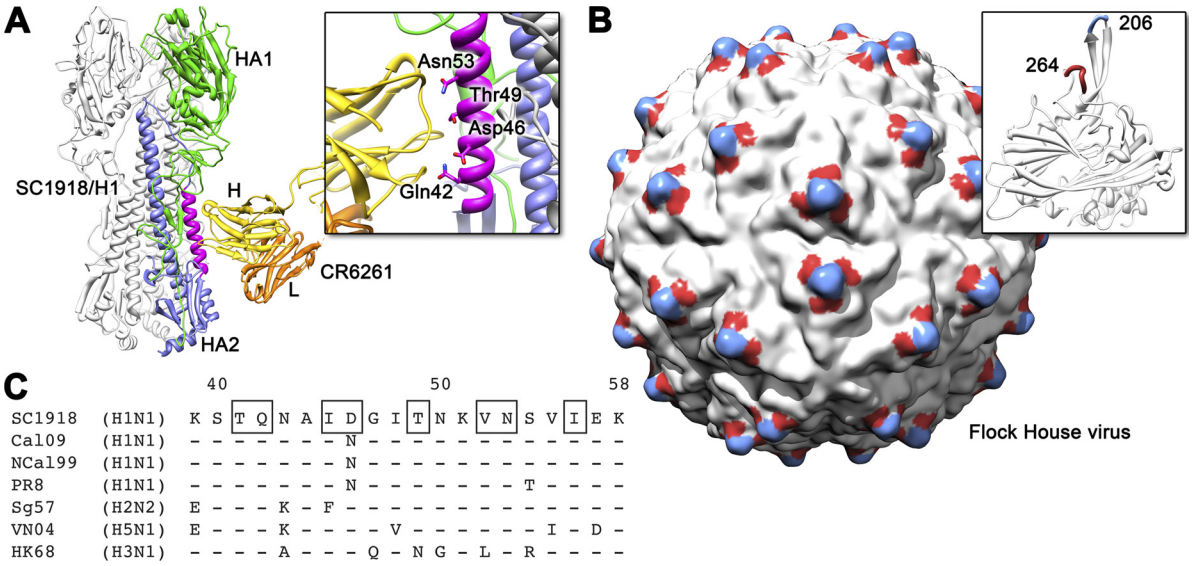

FIG 1 Location and sequence conservation of a broadly immunogenic epitope in HA and positions on the FHV capsid chosen for antigen display. (A) Structure of the SC1918/H1 influenza virus hemagglutinin (HA) bound by the broadly neutralizing antibody CR6261 (12). Trimeric HA is shown as a ribbon diagram with only one monomer shown in color for clarity (HA1 and HA2 chains are green and blue, respectively). The membrane-proximal region is at the bottom, and the solvent-exposed HA1 head is at the top. CR6261 bound to the colored HA monomer is shown as a ribbon diagram with the heavy and light chains shown in yellow and orange, respectively. The short HA2 A-helix (magenta) constitutes the major part of the epitope, and exposed residues are specifically bound by the CR6261 heavy chain (inset). (B) Surface structure of the FHV capsid showing the 60 locations where two protein loops reside that can be targeted for genetic insertion or replacement (blue, 206 loop; red, 264 loop). The two loops represent the most exposed regions of the capsid protein (inset), and three of each are present at the 60 sites. This allows a total of 180 copies of a foreign peptide or protein to be displayed with icosahedral symmetry when substituted for one of the loops. (C) Alignment of A-helix sequences from different HA subtypes and viral strains used in the present study. Residues 39 to 58 of the HA2 chain are shown. From top to bottom, complete viral strain designations are as follows: A/South Carolina/1/1918, A/California/7/09, A/New Caledonia/20/99, A/Puerto Rico/8/34, A/Singapore/1/57, A/Vietnam/1203/04, and A/Hong Kong/1/68. Boxed amino acids in the top sequence indicate residues that make contact with CR6261.

tions. Thus, it has been proposed that the A-helix alone may be sufficient as an antigen to induce antibodies with neutralizing specificity equivalent to that of CR6261 (12).

To test this hypothesis, we developed a general strategy for multivalent display of short helical peptides on the surface of FHV VLPs. Here, we report the synthesis and structural characterization of chimeric FHV VLPs that display 180 copies of the A-helix on their surfaces. We evaluated immunogenicity of the chimeric particles in mice and examined the antibody response to the A-helix. Our results demonstrate that, in the context of the engineered VLPs, the A-helix is sufficient for generating an antibody response against a range of hemagglutinin subtypes in group 1, but these antibodies are unable to neutralize influenza virus.

MATERIALS AND METHODS

VLP and antigen design. Two small loops on the FHV particle surface (PDB 2Z2Q), coat protein residues 206 to 208 and 264 to 268, are amenable to insertion of foreign proteins without affecting subsequent assembly into icosahedral particles (10, 24). In the first step, the programs Coot (14) and Chimera (29) were used to splice the structure of helix-turn-helix protein B2 (PDB 2AZ2 and 2AZ0) into the structure of the FHV capsid subunit in place of the 206 or 264 loops. The residues near the B2 termini in the best locations to start and end the inserts (i.e., unstructured polypeptide), while maintaining exposure and structure of the B2 helical segments, were identified. To display the antigenic helix identified in the structures of the CR6261-HA complexes (PDB 3GBN and 3GBM) (12), a portion of the long helix in B2 (residues 40 to 59) was then replaced with the HA2 A-helix (residues 39 to 58) from the human 1918 H1N1 pandemic virus (A/South Carolina/1/1918, PDB 3GBN). The A-helix was specifically oriented within the B2 helical turns so that residues in contact with the CR6261 antibody had maximum solvent exposure on the surface of the engineered coat protein. Thus, the HA2 A-helix is presented as part of a nested set of scaffolds where the A-helix is incorporated into the B2 scaffold, and the B2-A-helix scaffold is incorporated into the virus coat protein. Secondary structure prediction of the resulting chimeric protein sequences by the PsiPred server (5) was used to determine the likelihood of retaining the helix-turn-helix motif. The coordinates for the full icosahedral particles were then generated and analyzed for any potential properties that would interfere with assembly of the VLP or display of the inserted antigens. The CR6261 Fab was docked to the chimeric particle models, by superimposing the A-helices from each structure, to verify accessibility of the epitope on the modified particle surface.

Cloning, expression, and purification of VLPs. DNA fragments encoding FHV coat protein chimeras containing the HA2 A-helix and segments of FHV protein B2 were generated by overlap-extension PCR. Three DNA fragments encompassing the nucleotide sequence for the N-terminal portion of the FHV coat protein (residues 1 to 206), B2 protein (residues 3 to 63), and the C-terminal portion of the FHV coat protein (residues 209 to 407) were initially generated. The template used for generating segments containing the FHV coat protein sequences was plasmid p2BSwt (34), which contains the cDNA of FHV RNA2. The template used for generating the segment containing the B2 protein sequence was pFHV(1,0) (1), which contains the cDNA of FHV RNA1. The fragments were spliced together in the order $FHV_{N\text{-}term}$-B2-$FHV_{C\text{-}term}$ by overlap-extension PCR, and the product was digested with BamHI and XbaI and ligated into equally digested pBacPAK9 (BD Biosciences). The resulting plasmid was amplified in *Escherichia coli* and served as a template for replacing residues 40 to 59 of B2 protein with residues 39 to 58 of influenza virus HA2 from the human 1918 H1N1 pandemic virus (A/South Carolina/1/1918) (SC1918 strain). To this end, a second round of overlap-extension PCR was performed with primers that incorporated the sequence of HA2 residues 39 to 58 in their 5′ and 3′ extensions. The final product, referred to as FHV_{206}-B2-HA, sequentially encoded FHV coat

protein residues 1 to 206, B2 residues 3 to 39, HA2 residues 39 to 58 (the A-helix), B2 residues 60 to 63, and FHV coat protein residues 209 to 407. An analogous strategy was used to generate clone FHV_{264}-B2-HA, which sequentially encoded FHV coat protein residues 1 to 264, B2 residues 3 to 39, HA2 residues 39 to 58, B2 residues 60 to 63, and FHV coat protein residues 268 to 407. All plasmids were sequenced to confirm presence of the correct nucleotide sequences. Recombinant baculoviruses were generated by transfecting Sf21 cells with a mixture pBacPAK9 containing the sequence for either FHV_{206}-B2-HA or FHV_{264}-B2-HA and Bsu36I-linearized BacPAK6 (BD Biosciences) baculovirus DNA as described previously (40).

To generate VLPs, Sf21 cells were infected with recombinant baculovirus at an MOI of 0.5 to 1, and cultures were harvested at 3 days postinfection. Cells were pelleted at 1,500 × *g* for 10 min at 4°C and resuspended in 50 mM HEPES (pH 7) containing 1% (vol/vol) NP-40 and protease inhibitors (Roche) using 1/6 of the initial culture volume. Cells were lysed on ice for 10 min, and debris was pelleted at 13,774 × *g* for 10 min at 4°C. VLPs in the supernatant were pelleted through a 30% (wt/wt) sucrose cushion in 50 mM HEPES (pH 7) at 184,000 × *g* for 2.5 h at 11°C and resuspended in 50 mM HEPES (pH 7) containing protease inhibitors (Roche). Resuspended pellets were treated with RNase A for 30 min at 37°C and then centrifuged at 16,100 × *g* for 10 min at 4°C. The supernatant was loaded onto 10 to 40% (wt/wt) sucrose gradients in 50 mM HEPES (pH 7) and centrifuged at 197,568 × *g* for 1.5 h at 11°C. VLPs were harvested from the gradients by needle puncture and stored at −20°C.

Cloning, expression, and purification of HAs. Based on H3 numbering, cDNAs corresponding to residues 11 to 329 (HA1) and 1 to 176 (HA2) of the ectodomain of the HA were fused to an N-terminal gp67 signal peptide and to a C-terminal biotinylation site (amino acid sequence GGGLNDIFEAQKIEWHE), trimerization domain, and His tag by overlap PCR, essentially as previously described (12). The trimerization domain and His tag were separated from the HA ectodomain by a thrombin cleavage site. The resulting PCR products were digested with SfiI and inserted into a custom baculovirus transfer vector (pDCE066 or pDCE198). Recombinant bacmid was generated using the Bac-to-Bac system (Invitrogen), and virus was rescued by transfecting purified bacmid DNA into Sf9 cells using Cellfectin II (Invitrogen). HA protein was produced by infecting suspension cultures of Hi5 cells (Invitrogen) with recombinant baculovirus at an MOI of 5 to 10, followed by incubation at 28°C with shaking at 110 rpm. After 72 h, the cultures were clarified by two rounds of centrifugation at 2,000 × *g* and 10,000 × *g* at 4°C. The supernatant, containing secreted, soluble HA was concentrated and buffer exchanged into 1× phosphate-buffered saline (PBS; pH 7.4). After metal affinity chromatography using Ni-NTA resin, HAs were digested with trypsin (New England BioLabs; 5mU of trypsin per mg of HA, 16 h at 17°C) to produce uniformly cleaved (HA1/HA2) and to remove the trimerization domain and His tag. After the digests were quenched with 2 mM phenylmethylsulfonyl fluoride, the digested material was further purified by size-exclusion chromatography (10 mM Tris [pH 8.0], 150 mM NaCl).

Cryo-EM, data collection, and image reconstruction of VLPs. Frozen hydrated samples of purified VLPs at 5 mg ml^{-1} were prepared on C-flat CF-22-4C grids (Protochips). Briefly, a 5-μl sample was applied to a freshly plasma cleaned grid, and the grid was blotted for 5 s using an FEI Vitrobot instrument and quickly plunged into a bath of liquid ethane at −180°C. Grids were handled and stored under liquid nitrogen. Cryo-electron microscopy (cryo-EM) data were collected at the National Resource for Automated Molecular Microscopy using the LEGINON suite operating an FEI Tecnai F20 electron microscope (37). Images were collected at a nominal magnification of ×80,000, a defocus range of −1.2 to −2.5 μm, and a high tension of 120 kV onto a Gatan 4k-by-4k charge-coupled device (CCD). The pixel size of the CCD was calculated using the diffraction pattern from a 2D catalase crystal with known cell parameters. Contrast transfer function estimation was done with ctffind3 (27), and correction was done with ACE2 through the Appion package (22, 37). Particle picking was done using DoG Picker (41). A 25-Å resolution electron density map calculated from the deposited structure of FHV (PDB entry 2Q26) served as the starting model for image reconstruction using the EMAN package (23). The resolution of the image reconstructions, at a Fourier shell correlation of 0.5, was calculated to be 14 Å.

Cryo-EM model fitting. The original model coordinates for the chimeric FHV subunits were fitted into the moderate resolution particle density using the program Coot (14). The models were converted to polyserine residues for more flexible fitting. Coordinates for the majority of the FHV coat protein fit the density without modification. The insert at position 264 was disordered after the first few residues and was placed in random orientations in the final model for visualization purposes only. The insert at position 206 was fitted using a combination of real-space refinement and manual adjustments.

Immunization and viral challenge of mice. All animal procedures were performed in accordance with protocols approved by the Institutional Animal Care and Use Committees of The Scripps Research Institute or the Mount Sinai School of Medicine. In experiments 1 and 2 (see Fig. 4 and 5), 6- to 8-week-old male BALB/c mice (four to six animals per group; Scripps Breeding Colony) were injected subcutaneously with 100 μl of PBS containing 10 μg of VLP-206 or VLP-264. A control group received buffer only. All animals were immunized three times in intervals of 3 weeks. Mice were anesthetized with isoflurane before all procedures. Serum was prepared from whole blood collected from the submandibular vein prior to each injection as well as 2 weeks after the final immunization (week 8). In experiment 3 (Fig. 7), two groups of 6- to 8-week-old female BALB/c mice (five animals per group; The Jackson Laboratory) were immunized subcutaneously with 18 μg of wild-type FHV or VLP-264 infused with complete Freund adjuvant (MP Biomedicals, LLC). At 2 weeks after priming, mice were boosted with the same amount of particles infused with incomplete Freund adjuvant (MP Biomedicals, LLC). Serum was prepared from whole blood collected retro-orbitally 10 days after prime and boost immunizations. Mice were challenged via the intranasal route 2 weeks after the boost with five 50% mouse lethal doses (mLD_{50}) of mouse-adapted PR8 (H1) in a total volume of 20 μl. The body weight was monitored daily, and mice that lost more than 25% of their original body weight were sacrificed and marked as dead. In experiment 4 (Fig. 9), 6- to 8-week-old male BALB/c mice were immunized subcutaneously with 200 μl of a 1:1 mixture of PBS and Rehydragel (Rehis, Inc., Berkeley Heights, NJ) containing 10 μg of VLP-206 (PR8), VLP-264 (PR8), or 10 μg of each type of VLP. A control group received PBS-Rehydragel only. Animals were immunized three times at 3-week intervals. Serum was prepared from whole blood collected from the submandibular vein prior to each injection, as well as 2 weeks after the final immunization (week 8).

ELISA. Sera collected from mice in immunization experiments 1, 2, and 4 were tested using the enzyme-linked immunosorbent assay (ELISA) protocol described by Manayani et al. (24). Briefly, 0.5 to 1 μg of antigen (purified wild-type [wt] FHV VLPs, purified MBP-B2 fusion protein or purified, trypsin-cleaved trimeric HA) in 0.1 M $NaHCO_3$ was used to coat wells of a 96-well Immulon microtiter plate (Thermo Scientific) for 1 h at room temperature, followed by blocking overnight at 4°C in 3% nonfat milk in TBS (pH 7). Mouse sera were diluted 1:100, 1:1,000, or 1:10,000 in 1% nonfat milk in TBS with 0.05% Tween 20. Goat anti-mouse antibody coupled to horseradish peroxidase (HRP) was used as a secondary antibody, and antibody binding was quantified with TMB (3,3′,5,5′-tetramethylbenzidine) substrate. Color development was stopped after incubation for 10 min at 37°C by the addition of HCl, and signal was quantified by measuring the absorbance at 450 nm.

Sera collected from mice in experiment 3 were tested using the following ELISA protocol: purified HA (2.5 μg/ml) in PBS was used to coat the wells of a 96-well EIA/RIA plate (catalog no. 3590; Corning, Inc.) using 50 μl per well. Plates were incubated at 4°C overnight, washed three times with 0.1% Tween 20–1× PBS, and blocked with 200 μl of 5% nonfat milk–1× PBS for 30 min at room temperature. Serial dilutions of sera were added, and plates incubated for 2 h at room temperature. Plates were washed three times, an anti-mouse IgG-HRP secondary antibody (1:

5,000; NA931V; GE Healthcare) was added, and the plates were incubated for 1 h at 37°C. After the plates were washed three times, 200 μl of *o*-phenylenediamine dihydrochloride (Sigma) substrate was added, and the plates were read at 405 nm.

SDS-PAGE and immunoblot analysis. SDS-PAGE and immunoblot were carried out as described previously (11). Briefly, purified, trypsin-cleaved SC1918HA (1 μg) and wt FHV VLPs (1 μg) were electrophoresed through neighboring lanes of a 12% Laemmli gel and transferred to nitrocellulose. Transfer was performed overnight at 20 mA. Membranes were blocked in PBS containing 5% nonfat dry milk and then incubated with a 100-fold dilution of indicated mouse sera. The secondary antibody was HRP-conjugated goat anti-mouse (catalog no. 115-035071; Jackson Immunoresearch) used at a 1:4,000 dilution. Immune complexes were visualized by enhanced chemiluminescence (SuperSignal; Thermo Scientific) and exposure to X-ray film.

RESULTS

Design and synthesis of VLPs displaying the influenza virus A-helix. The A-helix forms the major part of a functionally conserved epitope in the membrane proximal stalk of influenza virus HA. To elicit a potent antibody response against this helix, we chose to present it to the immune system in a polyvalent manner on the surfaces of FHV VLPs, which are known to be highly immunogenic (24). Two small loops on the FHV particle surface, residues 206 to 208 and residues 264 to 268 (Fig. 1B), were chosen as exogenous protein insertion sites based on several key properties: high solvent exposure, trimeric arrangement (particularly position 206) after particle assembly, flexible polypeptide termini in close proximity after the loops are removed, and proven ability to accommodate insertions without affecting particle assembly. Simply inserting the A-helix coding sequence (KSTQNAIDGITN KVNSVIEK) into these surface loops, however, was unlikely to preserve its helical conformation. We therefore selected protein B2, a small helix-turn-helix nonstructural protein also encoded by FHV (6), as a scaffold for maintaining the secondary structure of the A-helix peptide (Fig. 2A). The B2 scaffold added two vertically oriented helices ~40 Å in length to the solvent-exposed surface of each coat protein subunit. A portion of the long helix in B2 was then replaced with the 20-residue peptide comprising the A-helix of HA from the human 1918 H1N1 pandemic virus (A/South Carolina/1/1918) (Fig. 2B). The A-helix was positioned with respect to the B2 helical turns in order to maximize solvent exposure of the CR6261 contact residues by putting them on the outward facing surfaces of the insert (Fig. 2C). Coordinates for the designed B2/A-helix chimera were then inserted at FHV positions 206 and 264 (Fig. 2D), and models of the full icosahedral particles were generated. Evaluation of the particle models showed no potential properties that would interfere with assembly of the VLP or display of the inserted antigens. The inserts were expected to be vertically oriented at position 206 due to their close proximity to one another (~8 Å) and the native β-strands that start the loop. Although no changes to the virus or insert sequences were made to promote interactions between them, we were aspiring to produce a trimeric stem-like structure by placing them at the quasi-3-fold axes of the particle. The inserts at position 264 are 10 Å farther from the quasi-3-fold axis, which separates them ~14 Å from one another, with the native 206-208 loops forming a knob structure centered between them. Therefore, well-ordered interactions between the B2/A-helix inserts at position 264 were considered unlikely.

The final designs were used to generate cDNA clones of the chimeric FHV coat proteins containing the B2/A-helix fragment at either insertion point. The two chimeras were expressed in insect cells using recombinant baculovirus vectors. Both modified proteins readily assembled into spherical, intact, and homogeneous VLPs displaying 180 copies of the A-helix (Fig. 2E and F). Consistent with predictions from the modeling studies, negatively stained particles viewed in the electron microscope had an uneven, somewhat jagged surface and a slightly larger diameter compared to wild-type FHV particles.

Structure of the chimeric VLPs. Cryo-EM analysis and image reconstruction of the VLPs at 14-Å resolution showed that the inserts at the 206 site (Fig. 2G) created a new trimeric spike ~50 Å in height at the substitution sites. The size and shape of the trimeric structure indicated that each spike was composed of three copies of the insert and that they had established fortuitous interhelical contacts to stabilize their vertical protrusion from the particle surface. The spikes made contact at their distal tips across the particle 2-fold axes, which also may have stabilized their rigid structures but, consequently, blocked access to one of the A-helix sites in each spike.

The initial model of VLPs with the insert at position 206 (hereafter referred to as VLP-206) (Fig. 2D) was fitted into the image reconstruction using a combination of automated and manual procedures in order to obtain its actual structure and provide a basis for interpreting the resulting immunogenic properties of the inserted B2/A-helix antigen. The resulting fit of the position 206 particle density (Fig. 3A and B) indicated that the inserts twist about each other slightly at their midpoints, and the exposed tips point outward resulting in a slight bend of the A-helix. Importantly, the fit to density indicated that the B2/A-helix insert had retained its helical structure and exposed the A-helix on two of the three faces of the spike in the VLP-206 particles.

In contrast, the reconstructed image of VLPs with the inserts at position 264 (hereafter referred to as VLP-264) (Fig. 2H) was closely similar to an unmodified FHV capsid (e.g., Fig. 1B), demonstrating that the inserts at the 264 site did not form any icosahedrally ordered structures. Instead, the lack of density indicated that they adopt diverse orientations across the surface of the particles. Fitting of coordinates representing the B2/A-helix insert was not possible at the 264 insertion site due to the disordered density; thus, the three inserts were each aligned differently in the VLP-264 model to visualize a particle with variably oriented inserts (Fig. 3C). It suggested the inserts formed an irregular, unstructured sheath over the VLP-264 surface, potentially giving the A-helix more varied and possibly greater exposure compared to the 206 particle. However, it was not possible to determine whether the epitope was helical or accessible on the 264 particle surface. Taken together, the B2/A-helix scaffold designs were successful in (i) creating correctly folded coat protein chimeras that then (ii) assembled into icosahedral particles and (iii) prominently displayed the B2/A-helix inserts at both the 206 and 264 sites, with the former adopting a trimeric oligomerization of the helices.

Monoclonal antibodies CR6261 (Fab fragment) and F10 (complete IgG) were used as tools to further probe the conformation of the inserts, but neither bound to the VLPs (data not shown). Given that these antibodies also failed to bind to a synthetic peptide representing the A-helix (data not shown), CR6261 and F10 may require additional HA1 and HA2 residues from their epitopes to form stable interactions with an antigen. Thus, the

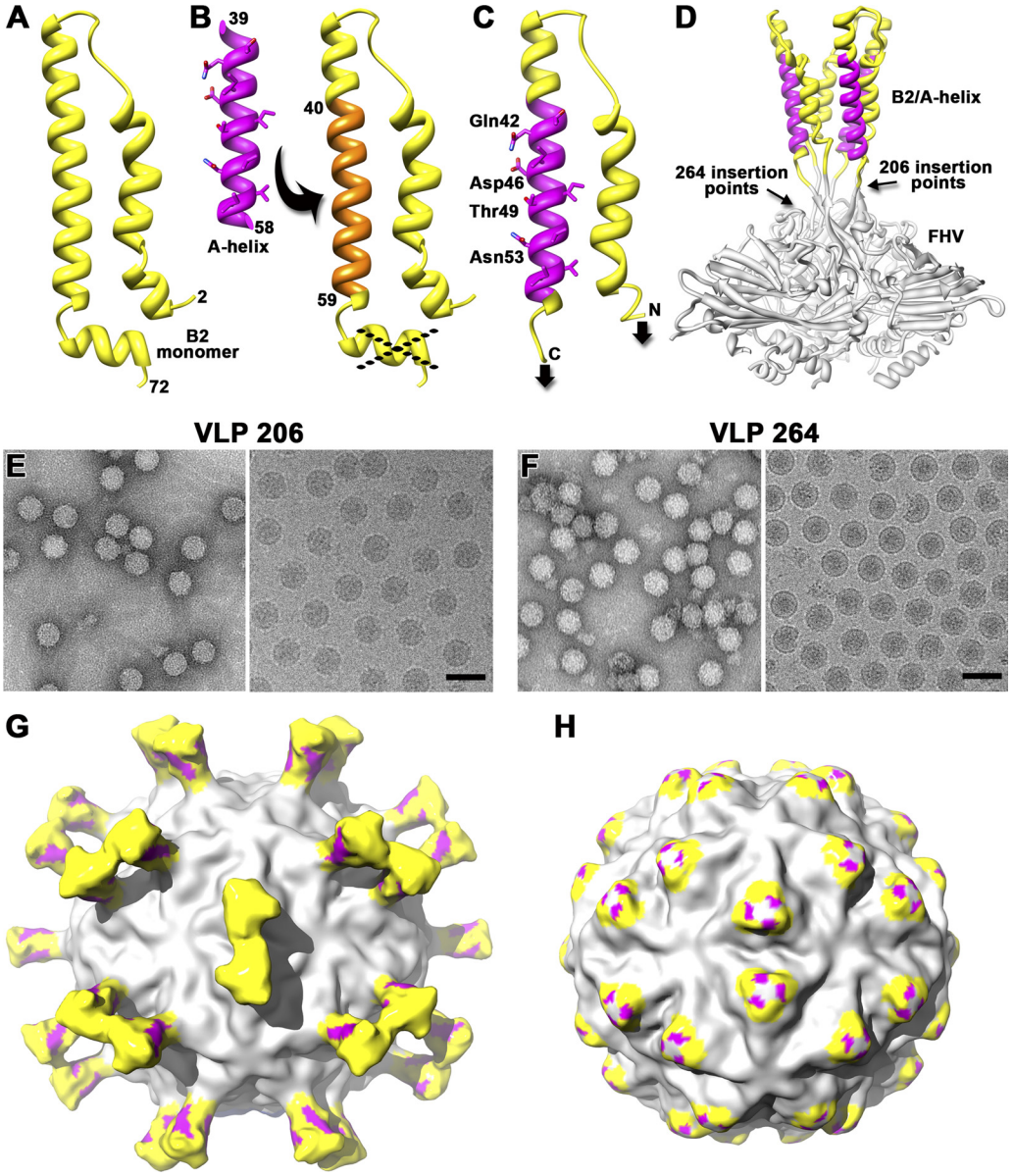

FIG 2 Design, construction, and structure of VLPs that multivalently display the influenza virus HA2 A-helix. (A) Monomer of the B2 protein shown as a ribbon diagram. Its small size and predominantly helical structure are valuable as a cassette for peptide substitutions. (B) The major antigenic site of the HA2 A-helix (magenta) is substituted for an equivalent length of helical residues in the long B2 helix (orange). B2 is slightly truncated to make the N and C termini meet at approximately the same position for insertion into loops. (C) The final B2/A-helix construct (yellow and magenta, respectively). The arrows denote the attachment points to the FHV capsid protein. (D) Trimer of modified FHV capsid proteins (gray) showing the complete design of the VLP with the B2/A-helix construct inserted at the 206 site. The 264 site is also marked. (E to H) Characterization and structure of particles produced after expression of the B2/A-helix construct inserted at the 206 (E and G) and 264 (F and H) sites of FHV. (E and F) Negative-stain (left) and cryo-EM (right) images of the 206 and 264 particles, respectively. The images show assembled icosahedral particles ~400 Å in diameter for both constructs. Scale bars, ~50 nm. (G and H) Image reconstructions of the 206 and 264 particles, respectively, at 14-Å resolution from the cryo-EM data (same color scheme as in panel D). The colored regions on the 264 particle (H) show where the inserts, if visible, would be positioned.

VLPs were expected to elicit anti-A-helix antibodies distinct from those of CR6261 or F10 since the particles did not display the complete epitope recognized by these antibodies.

Immune response to chimeric VLPs. BALB/c mice (four per group) were immunized three times in intervals of 3 weeks with 10 μg of purified VLP-206, VLP-264, or PBS as a control. No adjuvants were used in this study based on previous observations that the particles are strongly immunogenic (24). Blood was collected prior to each injection, as well as 2 weeks after the final boost, and serum was tested by ELISA for the presence of antibodies to FHV coat protein, B2 protein, and full-length, trimeric HA (SC1918/H1), the latter cleaved with trypsin to generate HA1/HA2 chains. Using trimeric HA as an antigen instead of A-helix peptide ensured that the assay was specific for detection of antibodies that, in principle, would be able to recognize the A-helix in the context of HA in its natural environment, such as influenza virus particles or

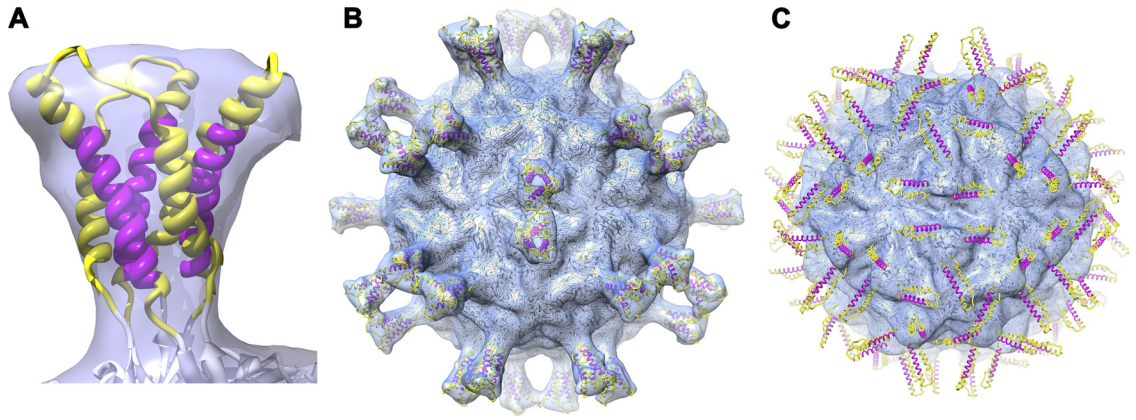

FIG 3 Fitted models of the VLP-206 and VLP-264 chimeras based on the cryo-EM image reconstructions in Fig. 2G and H (same coloring as in Fig. 2D). (A) Enlarged view of one set of inserts from a trimer fitted to the VLP-206 cryo-EM density map (transparent light blue). The volume of the density correlates well with the space required for three B2/A-helix scaffolds containing the epitope in a helical conformation. (B) The full VLP-206 map viewed down a particle 2-fold axis showing the complete set of fitted coordinates for the 180 modified coat proteins. The particle diameter is 430 Å. (C) The full VLP-264 map in the same orientation as in panel B also showing the complete set of fitted coat protein coordinates and random insert orientations. The particle diameter is 406 Å.

the plasma membrane of infected cells. As shown in Fig. 4, the A-helix displayed by VLP-264 was able to elicit IgG that recognized trimeric HA, whereas VLP-206 was not. Both types of particles induced rapid and potent antibody responses to FHV coat protein and the B2 scaffold regardless of the insert location.

The IgG responses were not uniform and reflected the structural differences between the modified particles. The response to FHV coat protein was stronger in mice immunized with VLP-206 than with VLP-264, whereas the opposite effect was observed for the response to the B2 scaffold. The vertically oriented spikes in VLP-206 leave large areas of the FHV capsid exposed and accessible to B cell receptors. Conversely, B cell receptor access to the spikes themselves may have been limited given the rigidity and close interaction of the inserts at the particle quasi-3-fold axes. Docking of the CR6261 antibody to the A-helices displayed in the fitted model of VLP-206 confirmed that the epitopes are not blocked, but that B cell receptors have a narrow range of available approaches due to the presence and close proximity of neighboring spikes on the particle surface. The highly flexible structure of the B2/A-helix inserts on VLP-264, on the other hand, may have caused the reverse effect by potentially forming a sheath over the surface of the underlying capsid. Such a cover would inhibit B cell

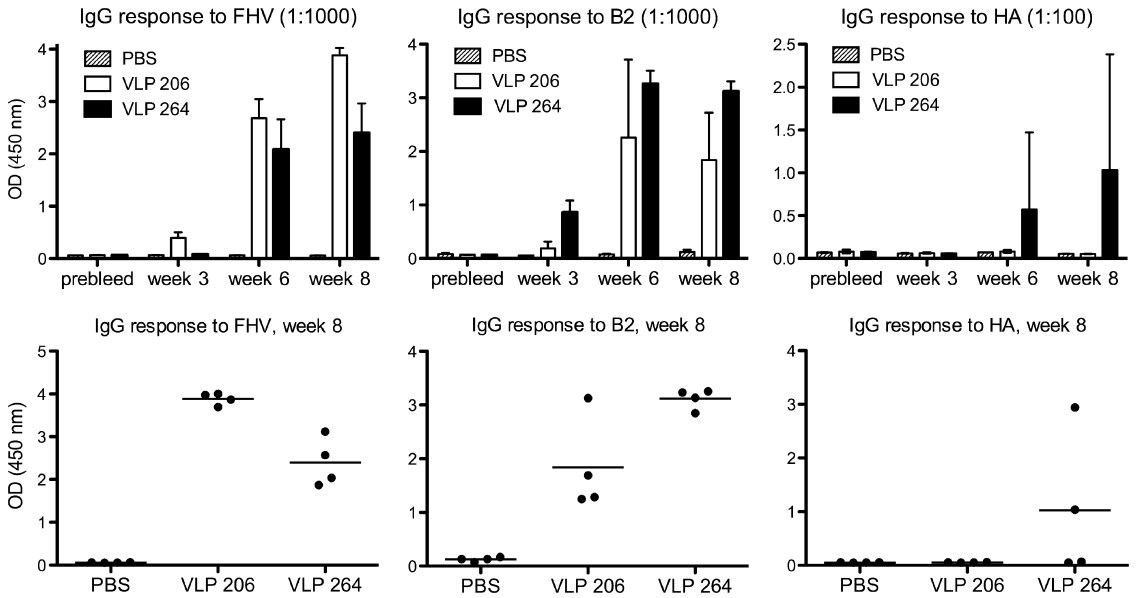

FIG 4 IgG-specific antibody response of mice vaccinated with FHV VLPs displaying the A-helix of SC1918 HA (H1). (Top row) Mice (four animals per group) were immunized subcutaneously with VLP-206, VLP-264, or PBS and boosted 3 and 6 weeks later. The presence of IgG to FHV coat protein, B2 protein, and cleaved, trimeric SC1918 HA in sera prior to immunization, as well as 3, 6, and 8 weeks postimmunization, was determined by ELISA using 1:1,000 (FHV, B2) and 1:100 (HA) serum dilutions. Bars represent average ELISA values for mice in each group. Error bars denote the standard deviation from the mean. Note that only two of four mice were positive for the presence of antibodies to HA, explaining the large error bars. (Bottom row) IgG levels of individual mice 8 weeks after immunization. The horizontal bar represents the average value for each group. Of the two animals whose sera reacted with HA in the VLP264 group, the one that gave the higher ELISA value is animal 9. The serum from this animal also reacted with denatured HA2 as shown in Fig. 6A.

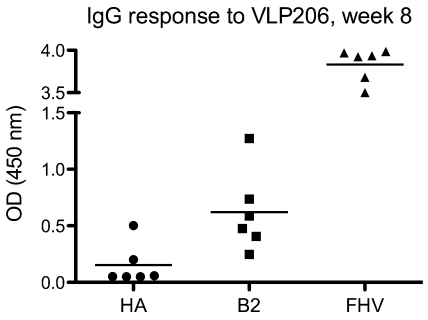

FIG 5 IgG-specific antibody response of mice vaccinated with VLP-206. Mice (six animals per group) were immunized subcutaneously with VLP-206 and boosted 3 and 6 weeks later. The presence of IgG to FHV coat protein, B2, and cleaved, trimeric SC1918 HA at 8 weeks postimmunization was determined by ELISA using 1:1,000 (FHV, B2) and 1:100 (HA) serum dilutions. The data points represent the antibody levels of individual mice, and the horizontal bar indicates the average value for each group.

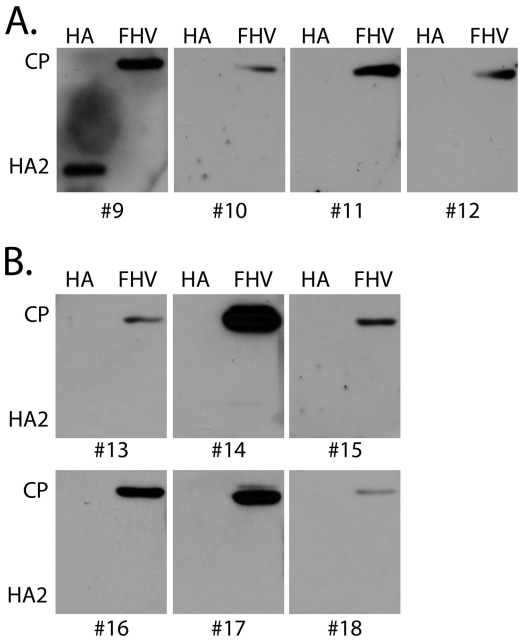

FIG 6 Immunoblot analysis to probe for the presence of antibodies that recognize denatured HA and FHV coat protein after immunization of mice with VLP-264 or VLP-206. Purified, trypsin-cleaved SC1918 HA (1 μg) and wt FHV VLPs (1 μg) were loaded in neighboring wells of a reducing, denaturing polyacrylamide gel and transferred to nitrocellulose membrane after electrophoresis. Individual membranes were blocked and then incubated with a 100-fold dilution of the same week 8 mouse sera for which ELISA results are shown in Fig. 4 and 5. Immune complexes were visualized by enhanced chemiluminescence after incubation of the blots with HRP-conjugated secondary antibodies. The numbers below each panel identify individual animals. (A) Week 8 sera from mice immunized with VLP-264. Only serum 9, which gave the highest value in ELISA shown in Fig. 4, contained antibodies that recognize denatured HA2. (B) Week 8 sera from mice immunized with VLP-206. The ELISA data for these sera are shown in Fig. 5.

interactions with the coat protein while simultaneously enhancing contact with the B2 epitopes presented in diverse orientations. Although highly flexible, the antibody response to both the B2 scaffold and trimeric HA proteins strongly suggested that the VLP-264 inserts retained the A-helix epitope structure and helix-turn-helix motif.

Compared to the IgG response against FHV coat protein and B2 protein, the response to the A-helix was considerably weaker and only detectable after mice had been boosted at least once. A modest increase in antibody titer was observed after the second boost. Indeed, only two of four mice immunized with VLP-264 generated IgG positive for trimeric HA, whereas no anti-HA IgG was detectable in mice immunized with VLP-206, although the structure and exposure of the A-helix was suitable to generate a response. To validate the VLP-206 design or verify it was incapable of eliciting anti-HA antibodies, a second group of mice was inoculated with VLP-206 following the same injection schedule. In this group, two of six mice generated antibodies to trimeric HA (Fig. 5). As with the VLP-264 results, the anti-HA titer was considerably lower than those against the FHV and B2 proteins. Thus, both VLPs were capable of eliciting an anti-HA IgG response in mice. Although nonuniform and relatively weak, it indicated that the A-helix is presented on the surface of both particles in a manner related to its structure and exposure in the HA stalk.

Nonetheless, to exclude the possibility that positive HA ELISA data reflected an antibody response to a linear, nonhelical A-peptide as a result of partial denaturation of HA antigen during the assay, week 8 sera from all animals were tested for reactivity against denatured HA and FHV coat protein by immunoblot analysis (Fig. 6). The sera reacted to various degrees with denatured FHV coat protein, indicating the presence of linear epitopes in the three-dimensional structure of the protein. In contrast, only one serum, that of animal 9, reacted with denatured HA2 (Fig. 6A). Taken together, these results support that both the VLPs presented the scaffolded A-helix in its native or near native conformation. However, the weak or negative responses of the mice to this helix point to other issues that may be related to the VLP designs, such as reduced immunogenicity of the A-helix in the context of the B2 scaffold.

VLP-elicited antibodies recognize multiple HA subtypes from group 1. The mouse immunization study was repeated with VLP-264 to further characterize the specificity of the antibodies induced against the A-helix. To this end, BALB/c mice (five animals per group) were immunized with either wt FHV as a control or VLP-264 in the presence of Freund adjuvant and boosted once 2 weeks after the first immunization. Ten days after primary and secondary immunizations, blood was collected and serum was tested by ELISA against trimeric HA representing group 1 subtypes H1 (Cal/09), H2 (Sg/57), and H5 (VN04) and group 2 subtype H3 (HK/68). In the present study, all five mice injected with VLP-264 showed measurable but still relatively weak responses against all tested group 1 subtypes, particularly after the boost (Fig. 7). There was no response against the H3 subtype in the inoculated mice or against any subtype by the control mice. These results correlated well with the specificities of broadly neutralizing antibodies CR6261 and F10, which neutralize group 1 influenza viruses but not group 2 viruses, and provided further evidence that the VLPs displayed the A-helix epitope in an authentic conformation. The inability of antibodies to interact with group 2 subtypes, such as H3, has been attributed to the glycosylation of nearby Asn38 of the HA1 chain blocking the A-helix epitope (12).

Sera containing A-helix antibodies do not neutralize influenza virus. Sera positive for the presence of anti-A-helix antibodies were tested in microneutralization assays for their ability to neutralize influenza virus strains A/New Caledonia/20/99 and

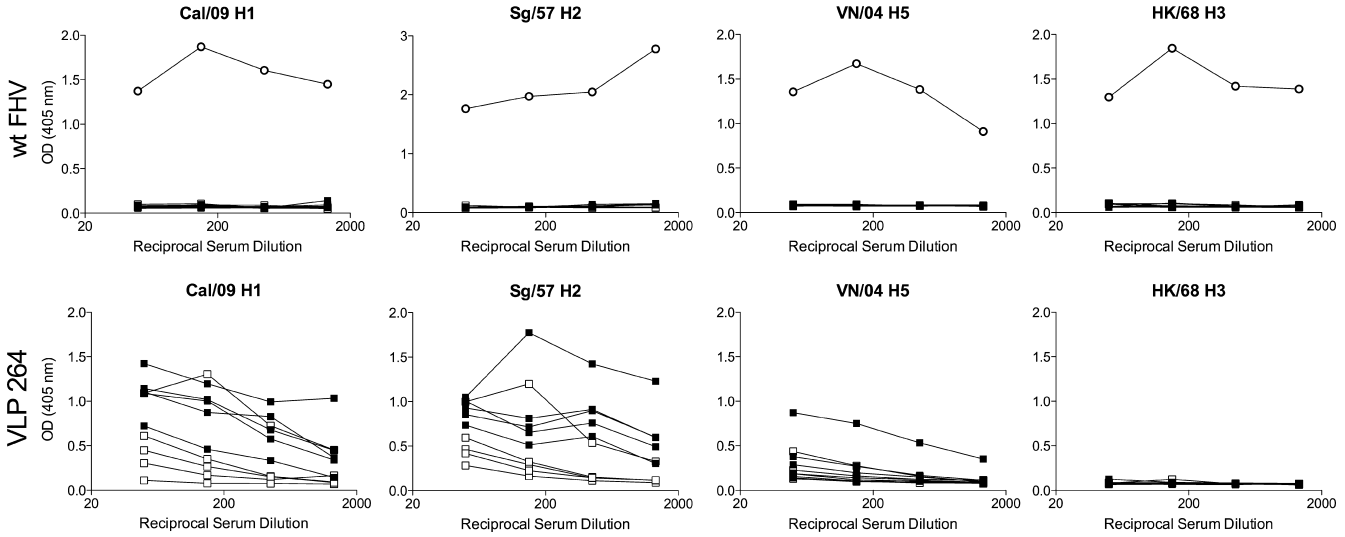

FIG 7 Immunization of mice with VLP-264 elicits antibodies that react with multiple HA subtypes. Mice (five animals per group) were vaccinated with wt FHV particles as a control or VLP-264 in the presence of Freund adjuvant and boosted 2 weeks later. Serum from individual mice was prepared 10 days after primary and secondary immunizations and serial dilutions were tested by ELISA for the presence of IgG antibodies against purified HA representing H1, H2, H3, and H5 subtypes. (Top row) Sera collected from mice immunized with wt FHV. Open circles (top panel only) represent data obtained with a positive control serum against the HA subtype indicated in each panel. (Bottom row) Sera from mice immunized with VLP-264. Open squares represent data obtained with sera prepared after primary immunization, and closed squares represent data obtained with sera after secondary immunization.

A/California/7/09 (both H1N1). Unexpectedly, none of the sera, even when used at a low 20-fold dilution, neutralized or reduced infectivity of either virus (data not shown). Moreover, there was minimal protection of VLP-264-immunized mice when challenged with the mouse-adapted strain A/Puerto Rico/8/34 (H1N1) (Fig. 8).

The inability of the sera to neutralize influenza virus both *in vitro* and *in vivo* prompted us to compare the amino acid sequence of the A-helix displayed on the VLPs to those of the HAs used in the ELISA, microneutralization, and mouse challenge assays. Except for the HA with the matching A-helix used as antigen in our initial ELISA experiments (Fig. 4 and 5), the A-helices in all other HAs contained at least one amino acid change relative to SC1918 HA (Fig. 1C). The most closely related HA of strains A/California/7/09 and A/New Caledonia/20/99 carried a substitution at position 46 that changed aspartate to asparagine (D46N). The side chain of Asp46 in both the SC1918/H1 and the Viet04/H5 HAs contributes a hydrogen bond and makes two van der Waals contacts with Ser31 in the CR6261 heavy-chain variable domain (12). If Asp46 in the VLPs established equally important contacts with the elicited anti-HA antibodies, and keeping in mind that the 20-residue A-helix is the only HA segment presented by the VLPs, a change to Asn might significantly reduce the affinity between the antibodies and trimeric HA and prevent neutralization of a virus carrying that change. Based on these considerations, we generated a second set of VLPs, in which the sequence of the A-helix was changed to that of the common mouse-adapted laboratory strain A/Puerto Rico/8/34 (PR8).

Immune response to VLPs displaying the A-helix of PR8. BALB/c mice (eight animals per group) were immunized three times in an interval of 3 weeks with 10 μg of either VLP-206(PR8), VLP-264(PR8), a mixture of both types of VLP, or PBS. Rehydragel was included as an adjuvant. Blood was collected prior to each injection and 2 weeks after the final boost in week 8. Only week 8 serum samples were tested by ELISA using trimeric PR8 HA as an antigen. As with the VLPs presenting the SC1918/H1 A-helix, the VLPs presenting the PR8 A-helix elicited antibodies that bound trimeric HA (Fig. 9A). Interestingly, the group of animals immunized with both types of particles showed a greater number of anti-A-helix responders and had a higher average titer.

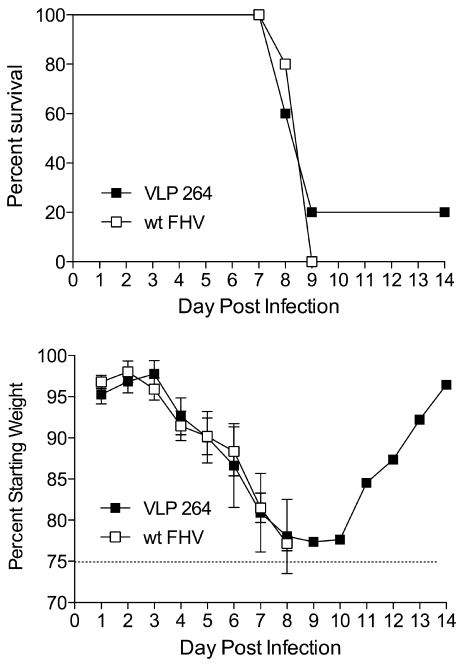

FIG 8 Immunization with VLP-264 does not protect mice from challenge with live virus. Mice (five animals per group) vaccinated with wt FHV or VLP-264 in the presence of Freund adjuvant and boosted 2 weeks later were challenged with 5 MLD_{50} of mouse-adapted H1 virus strain PR8 2 weeks after secondary immunization. Body weight was monitored daily, and mice that lost more than 25% of their original body weight were sacrificed and marked as dead. The immune responses of these mice to HA is shown in Fig. 7.

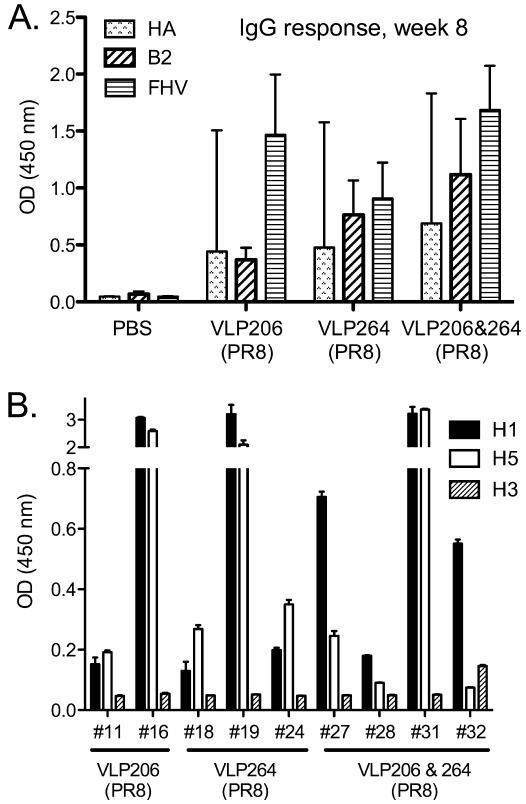

FIG 9 (A) IgG-specific antibody response of mice vaccinated with FHV VLPs displaying the A-helix of PR8 HA (H1). Mice (eight animals per group) were immunized subcutaneously with VLP-206 (PR8), VLP-264 (PR8), a mixture of both VLPs, or PBS and then boosted 3 and 6 weeks later. Rehydragel was included as an adjuvant. The presence of IgG to FHV coat protein, B2 protein, and cleaved, trimeric PR8 HA in sera prepared 8 weeks postimmunization was determined by ELISA using 1:10,000 (FHV, B2) and 1:100 (HA) serum dilutions. Bars represent the average ELISA values for mice in each group. Error bars denote the standard deviation from the mean. Note that one animal in the PBS group and one animal in the VLP-206/VLP-264 group died of unknown causes prior to blood collection in week 8. (B) Subtype specificity of anti-HA antibodies elicited in response to vaccination with VLPs displaying the A-helix of strain PR8. Sera containing antibodies against PR8 HA (H1) after immunization of mice with VLP-206 (PR8), VLP-264(PR8), or both types of VLPs were tested for binding to purified H5 and H3 HAs by ELISA using a 1:100 serum dilution. The horizontal axis identifies specific animals and the type of VLP with which they had been vaccinated. H5 HA was from strain A/Vietnam/1203/2004 and H3 HA was from strain A/Perth/16/2009. The data represent the mean of three independent measurements, and error bars denote the standard deviation from the mean.

Mouse sera that reacted with PR8 HA (H1) by ELISA were also tested for reactivity against H5 HA (group 1) and H3 HA (group 2). Except for one animal (animal 32), all sera recognized H5, but not H3 HA due to its glycosylation (Fig. 9B), consistent with the specificity expected for antibodies raised against the conserved exposed face of the A-helix. In immunoblot analysis, two of the nine positive sera, reacted weakly with denatured HA2 (animals 16 and 19), whereas one serum (animal 31) showed a stronger signal (data not shown). These results were consistent with previous observations that showed the VLPs displayed the A-helix in a near native conformation and that positive ELISA data could not generally be ascribed to the presence of antibodies that recognized denatured HA. However, despite these encouraging binding characteristics, the sera were unable to neutralize PR8 virus in a microneutralization assay (data not shown). Challenge of immunized animals with live virus was therefore not pursued.

DISCUSSION

Current efforts toward development of a universal influenza virus vaccine are broadly based on two strategies: the application of new approaches for delivery of existing vaccine constructs (43, 44) and the design of novel immunogens (3, 18, 35, 42). The former is exemplified by studies that used different hemagglutinins in sequential immunizations (43) or DNA and protein in a prime-boost regimen (44). Novel immunogens that have been tested include "headless" HA, in which the immunodominant, globular domain was removed from full-length HA (32, 35), and a synthetic peptide that represents the long central helix of the HA2 chain (42). Both strategies have shown encouraging results and may one day be used in combination.

We have used a structure-based approach to design an antigen that mimics the major determinant of a highly conserved epitope in the membrane-proximal stem of influenza virus hemagglutinin. Our work had two main objectives: first, to determine whether linear, helical epitopes can be presented as a stable structure on the surface of an icosahedral VLP and, second, to test the hypothesis that the A-helix of influenza virus HA is sufficiently immunogenic to induce broadly neutralizing antibodies.

Our strategy for synthesis of an effective A-helix antigen took into account that small peptides are poorly immunogenic and sample a variety of conformations instead of maintaining the secondary and tertiary structure of that segment in the corresponding protein. To enhance A-helix immunogenicity, it was genetically inserted into highly exposed protein loops on the exterior surface of VLPs derived from the insect virus FHV. The particulate nature and favorable dimensions of VLPs stimulate efficient uptake by antigen-presenting cells and transport to lymph nodes for presentation to cells of the adaptive immune system. VLPs also drain to lymph nodes independently of antigen-presenting cells to present conformation-dependent antigens to B cells (25). Finally, the VLP platform permits multivalent display of heterologous proteins and peptides, a feature known to improve immunogenicity by promoting cross-linking of B cell receptors.

To retain the secondary structure of the A-helix, we used the small helix-turn-helix protein B2 as a scaffold. The value of scaffolding proteins for presentation of epitopes in their native conformation has been demonstrated previously (7, 26, 28). B2 normally forms antiparallel homodimers that bind tightly to double-stranded RNA and inhibit RNA interference in FHV-infected cells (6). The structure of the monomer was ideally suited for insertion into the FHV loops because slight truncations brought its N and C termini into close enough proximity to match the distance between FHV loop residues to which connections had to be made. Also, there are no specific interactions between the hydrophobic residues lining the inner surfaces of the long and short helices in monomeric B2, suggesting that helical segments could be exchanged without disrupting the hairpin motif. Cryo-EM analysis and image reconstruction of the chimeric VLPs revealed the VLP-206 inserts retained the helix-turn-helix motif as highly exposed vertical columns on the particle surface. In contrast, the VLP-264 inserts had random orientations and yet were also able to elicit antibodies that recognized trimeric HA and B2 proteins, providing strong evidence that the inserts maintained the helix-turn-helix motif.

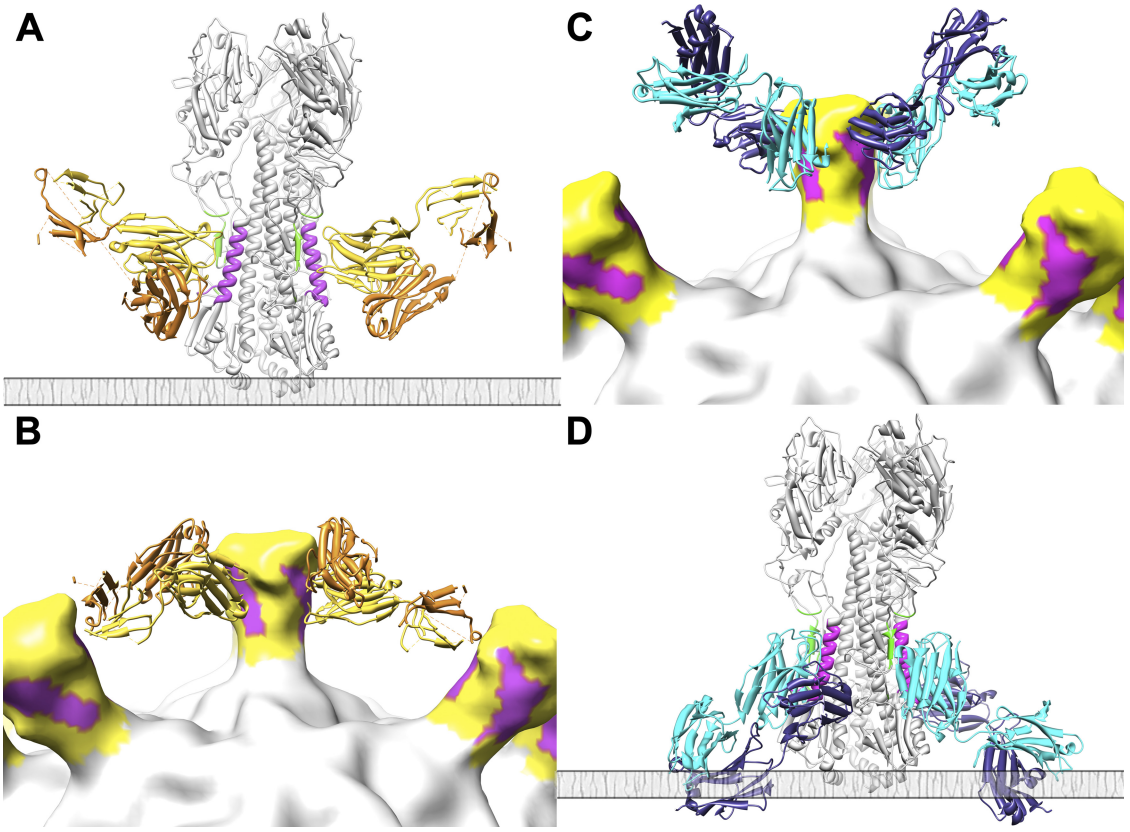

FIG 10 Comparison of antibody angles of approach imposed by native HA versus the VLP-206 presented A-helices. (A) Structure of the native SC1918-CR6261 complex as depicted in Fig. 1A with the viral membrane depicted below as a gray bar. Two bound antibodies are shown to demonstrate their angle of approach acts to prevent steric hindrance by the viral membrane. (B) Structure of VLP-206 as depicted in Fig. 2G with two CR6261 antibodies docked to the presented A-helix segments on one of the engineered spikes. Note the flip of the heavy and light chains due to the inversed orientation of the A-helix in VLP-206 relative to the particle surface. The antibodies remain roughly in a horizontal orientation with enough clearance for binding, but in what would be a stressed angle of approach for a B-cell receptor. (C) Model of a more probable angle of approach for antibodies generated against the VLP-206 presented A-helix. With a more acute angle of approach, the antibodies would have greater clearance and flexibility for antigen binding such as that seen by CR6261 to the HA stalk. (D) The antibodies generated by VLP-206 would be unable to bind to the HA associated with the viral membrane. The orientation of the A-helix is reversed in native HA relative to the VLPs; thus, the antibody orientations are also reversed and would have to approach the HA stalk through the membrane for optimal binding. The angles of approach to the VLP-264 presented helices would be analogous since the flexibility of the inserts does not compensate for the inverse orientation of the A-helices, even if they are laying flat across the particle surface.

We vaccinated mice with the two types of VLP using various immunization schedules and amounts of antigen in the presence or absence of two kinds of adjuvant. We collected blood at different times after primary and secondary injections. The IgG response to FHV coat protein and scaffolding protein B2 was consistently rapid and robust, whereas the response to the A-helix was slow, much weaker, and nonuniform. Although both types of particles elicited anti-A-helix antibodies, VLP-264 produced higher responses perhaps due to the flexible nature of the insert at that site or because some A-helices in VLP-206 are partially blocked due to the interaction of the inserts across the 2-fold axes of symmetry. Enhanced immunogenicity of flexible epitopes relative to rigidly displayed epitopes has been observed previously for protein scaffolds displaying the MPER epitope of HIV-1 gp41 (28).

We used trimeric, fully cleaved HA (i.e., HA1/HA2, not HA0) in ELISAs to probe for the presence of anti-A-helix antibodies. This was based on the assumption that such antibodies would also bind to HA in its native environment, such as influenza virus particles or HA on the surface of virus-infected cells. However, given the weak response, we were concerned that this strategy underestimated the true level of anti-A-helix antibodies if a significant portion had been elicited to non-native A-helix conformations. This possibility could be largely excluded, however, by demonstrating that, with few exceptions, sera were negative for binding to denatured HA2 by immunoblot analysis. Instead, anti-A-helix antibodies elicited by VLPs appeared to be structurally specific for the A-helices in natively folded HA molecules.

The notion that anti-A-helix antibodies elicited in response to vaccination with VLPs were structurally specific for the same A-helix conformation as monoclonal antibodies CR6261 and F10 was further supported by the observation that they reacted with HAs representing different subtypes in phylogenetic group 1, such as H1, H2, and H5, but not group 2, such as H3. However, in contrast to CR6261 and F10, the anti-A-helix antibodies did not neutralize influenza virus *in vitro*, nor did they protect immunized mice from challenge with live virus. The reason for this discrepancy is not yet known, and a detailed understanding will have to await isolation of monoclonal anti-A-helix antibodies and characterization of their interaction with HA. Based on current data, a simple explanation would be that serum levels of the required

antibodies were insufficient. Alternatively, low affinity or avidity of the antibodies or potential steric restrictions could form the basis for the lack of neutralization. For example, the anti-A-helix antibodies may have established additional contacts with the B2 scaffold. Inability to form analogous contacts in the context of HA would necessarily lower binding affinity between antibody and antigen. This problem could be addressed by trimming the B2 scaffold to the minimally required fragment necessary to maintain the conformation of the A-helix.

Alternatively, steric hindrance may have prevented anti-A-helix antibodies from making stable contacts with HA in its natural environment. For example, VLPs and HA display the A-helix in opposite orientations relative to the surfaces from which they project, i.e., the FHV and influenza virus particles, respectively. A possible consequence of this is that antibodies may use an angle of approach to contact the A-helix on VLPs that makes it impossible for them to access the A-helix in the context of HA that is anchored to a viral or cellular membrane (Fig. 10). If so, this problem could be resolved by transferring the A-helix in the VLP to the opposite side of the helix-turn-helix scaffold in order to reverse its orientation. That said, given the weak and inconsistent antibody response to the A-helix in immunized mice, it will also be important to investigate whether presentation of helical epitopes in a vertical helix-turn-helix motif impedes interaction of B cell receptors with the helix of interest, thereby resulting in poor overall responses.

Finally, we cannot exclude the possibility that the A-helix alone is not sufficient as an antigen to induce broadly neutralizing antibodies. Incorporating additional regions of the CR6261 epitope into the VLP display platform will test this possibility.

ACKNOWLEDGMENTS

This study was supported by grants from the National Institutes of Health to A.S. (AI92280) and to I.A.W. (AI058113), a predoctoral fellowship from the Achievements Rewards for College Scientists Foundation and the NIH Molecular Evolution Training Program GM080209 (D.C.E.), and the Skaggs Institute for Chemical Biology. Cryo-EM and image reconstructions were conducted at the National Resource for Automated Molecular Microscopy, which is supported by the National Institutes of Health through the National Center for Research Resource P41 program (RR17573).

REFERENCES

1. **Ball LA.** 1995. Requirements for the self-directed replication of flock house virus RNA 1. J. Virol. **69**:720–727.
2. **Barbey-Martin C, et al.** 2002. An antibody that prevents the hemagglutinin low pH fusogenic transition. Virology **294**:70–74.
3. **Bommakanti G, et al.** 2010. Design of an HA2-based *Escherichia coli* expressed influenza immunogen that protects mice from pathogenic challenge. Proc. Natl. Acad. Sci. U. S. A. **107**:13701–13706.
4. **Brown WL, et al.** 2002. RNA bacteriophage capsid-mediated drug delivery and epitope presentation. Intervirology **45**:371–380.
5. **Bryson K, et al.** 2005. Protein structure prediction servers at University College London. Nucleic Acids Res. **33**:W36–W38.
6. **Chao JA, et al.** 2005. Dual modes of RNA-silencing suppression by Flock House virus protein B2. Nat. Struct. Mol. Biol. **12**:952–957.
7. **Correia BE, et al.** 2010. Computational design of epitope-scaffolds allows induction of antibodies specific for a poorly immunogenic HIV vaccine epitope. Structure **18**:1116–1126.
8. **Corti D, et al.** 2010. Heterosubtypic neutralizing antibodies are produced by individuals immunized with a seasonal influenza vaccine. J. Clin. Invest. **120**:1663–1673.
9. **Corti D, et al.** 2011. A neutralizing antibody selected from plasma cells that binds to group 1 and group 2 influenza A hemagglutinins. Science **333**:850–856.
10. **Destito G, Schneemann A, Manchester M.** 2009. Biomedical nanotechnology using virus-based nanoparticles. Curr. Top. Microbiol. Immunol. **327**:95–122.
11. **Dong XF, Natarajan P, Tihova M, Johnson JE, Schneemann A.** 1998. Particle polymorphism caused by deletion of a peptide molecular switch in a quasiequivalent icosahedral virus. J. Virol. **72**:6024–6033.
12. **Ekiert DC, et al.** 2009. Antibody recognition of a highly conserved influenza virus epitope. Science **324**:246–251.
13. **Ekiert DC, et al.** 2011. A highly conserved neutralizing epitope on group 2 influenza A viruses. Science **333**:843–850.
14. **Emsley P, Lohkamp B, Scott WG, Cowtan K.** 2010. Features and development of Coot. Acta Crystallogr. D Biol. Crystallogr. **66**:486–501.
15. **Fleury D, et al.** 1999. A complex of influenza hemagglutinin with a neutralizing antibody that binds outside the virus receptor binding site. Nat. Struct. Biol. **6**:530–534.
16. **Fleury D, Daniels RS, Skehel JJ, Knossow M, Bizebard T.** 2000. Structural evidence for recognition of a single epitope by two distinct antibodies. Proteins **40**:572–578.
17. **Fleury D, Wharton SA, Skehel JJ, Knossow M, Bizebard T.** 1998. Antigen distortion allows influenza virus to escape neutralization. Nat. Struct. Biol. **5**:119–123.
18. **Hashem AM, et al.** 2010. Universal antibodies against the highly conserved influenza fusion peptide cross-neutralize several subtypes of influenza A virus. Biochem. Biophys. Res. Commun. **403**:247–251.
19. **Jennings GT, Bachmann MF.** 2008. The coming of age of virus-like particle vaccines. Biol. Chem. **389**:521–536.
20. **Kashyap AK, et al.** 2008. Combinatorial antibody libraries from survivors of the Turkish H5N1 avian influenza outbreak reveal virus neutralization strategies. Proc. Natl. Acad. Sci. U. S. A. **105**:5986–5991.
21. **Kusov YY, et al.** 2007. Immunogenicity of a chimeric hepatitis A virus (HAV) carrying the HIV gp41 epitope 2F5. Antivir. Res. **73**:101–111.
22. **Lander GC, et al.** 2009. Appion: an integrated, database-driven pipeline to facilitate EM image processing. J. Struct. Biol. **166**:95–102.
23. **Ludtke SJ, Baldwin PR, Chiu W.** 1999. EMAN: semiautomated software for high-resolution single-particle reconstructions. J. Struct. Biol. **128**: 82–97.
24. **Manayani DJ, et al.** 2007. A viral nanoparticle with dual function as an anthrax antitoxin and vaccine. PLoS Pathog. **3**:1422–1431. doi:10.1371/journal.ppat.0030142.
25. **Manolova V, et al.** 2008. Nanoparticles target distinct dendritic cell populations according to their size. Eur. J. Immunol. **38**:1404–1413.
26. **McLellan JS, et al.** 2011. Design and characterization of epitope-scaffold immunogens that present the motavizumab epitope from respiratory syncytial virus. J. Mol. Biol. **409**:853–866.
27. **Mindell JA, Grigorieff N.** 2003. Accurate determination of local defocus and specimen tilt in electron microscopy. J. Struct. Biol. **142**:334–347.
28. **Ofek G, et al.** 2010. Elicitation of structure-specific antibodies by epitope scaffolds. Proc. Natl. Acad. Sci. U. S. A. **107**:17880–17887.
29. **Pettersen EF, et al.** 2004. UCSF Chimera: a visualization system for exploratory research and analysis. J. Comput. Chem. **25**:1605–1612.
30. **Powilleit F, Breinig T, Schmitt MJ.** 2007. Exploiting the yeast L-A viral capsid for the in vivo assembly of chimeric VLPs as platform in vaccine development and foreign protein expression. PLoS One **2**:e415. doi: 10.1371/journal.pone.0000415.
31. **Pumpens P, Grens E.** 2001. HBV core particles as a carrier for B cell/T cell epitopes. Intervirology **44**:98–114.
32. **Sagawa H, Ohshima A, Kato I, Okuno Y, Isegawa Y.** 1996. The immunological activity of a deletion mutant of influenza virus haemagglutinin lacking the globular region. J. Gen. Virol. **77**:1483–1487.
33. **Schneemann A, Reddy V, Johnson JE.** 1998. The structure and function of nodavirus particles: a paradigm for understanding chemical biology. Adv. Virus Res. **50**:381–446.
34. **Schneemann A, Zhong W, Gallagher TM, Rueckert RR.** 1992. Maturation cleavage required for infectivity of a nodavirus. J. Virol. **66**:6728–6734.
35. **Steel J, et al.** 2010. Influenza virus vaccine based on the conserved hemagglutinin stalk domain. mBio **1**:e00018–10. doi:10.1128/mBio.00018-10.
36. **Sui J, et al.** 2009. Structural and functional bases for broad-spectrum neutralization of avian and human influenza A viruses. Nat. Struct. Mol. Biol. **16**:265–273.
37. **Suloway C, et al.** 2005. Automated molecular microscopy: the new Leginon system. J. Struct. Biol. **151**:41–60.
38. **Thiery R, et al.** 2006. Induction of a protective immune response against

viral nervous necrosis in the European sea bass *Dicentrarchus labrax* by using betanodavirus virus-like particles. J. Virol. **80**:10201–10207.
39. **Throsby M, et al.** 2008. Heterosubtypic neutralizing monoclonal antibodies cross-protective against H5N1 and H1N1 recovered from human IgM+ memory B cells. PLoS One **3**:e3942. doi:10.1371/journal.pone.0003942.
40. **Venter PA, Krishna NK, Schneemann A.** 2005. Capsid protein synthesis from replicating RNA directs specific packaging of the genome of a multipartite, positive-strand RNA virus. J. Virol. **79**:6239–6248.
41. **Voss NR, Yoshioka CK, Radermacher M, Potter CS, Carragher B.** 2009. DoG Picker and TiltPicker: software tools to facilitate particle selection in single particle electron microscopy. J. Struct. Biol. **166**:205–213.
42. **Wang TT, et al.** 2010. Vaccination with a synthetic peptide from the influenza virus hemagglutinin provides protection against distinct viral subtypes. Proc. Natl. Acad. Sci. U. S. A. **107**:18979–18984.
43. **Wang TT, et al.** 2010. Broadly protective monoclonal antibodies against H3 influenza viruses following sequential immunization with different hemagglutinins. PLoS Pathog. **6**:e1000796. doi:10.1371/journal.ppat.1000796.
44. **Wei CJ, et al.** 2010. Induction of broadly neutralizing H1N1 influenza antibodies by vaccination. Science **329**:1060–1064.
45. **Wrammert J, et al.** 2011. Broadly cross-reactive antibodies dominate the human B cell response against 2009 pandemic H1N1 influenza virus infection. J. Exp. Med. **208**:181–193.